GEODYNAMICS & TECTONOPHYSICS
Published by the Institute of the Earth's Crust, Siberian Branch, Russian Academy of Sciences

RECENT GEODYNAMICS

2026 VOLUME 17 ISSUE 1 ARTICLE 0877

ISSN 2078-502X

DOI: 10.5800/GT-2026-17-1-0877

DETERMINATION OF THE LOCAL MAGNITUDE SCALE (M_L) FOR MONGOLIA

B. Ganbat ✉, **U. Munkhuu**

Institute of Astronomy and Geophysics, Mongolian Academy of Sciences, Ulaanbaatar 13343, Mongolia

ABSTRACT. Adjusting the local magnitude scale to match the regional tectonic characteristics is crucial to enhance studies focused on evaluating seismic risk and measuring seismic activity in geologically dynamic zones. In this study, we developed a local magnitude scale for Mongolia. Using the Mongolia earthquake catalog for the period from 2012 to 2019, we analyzed 261 earthquakes with magnitudes >3.5 that occurred within a 1000 km epicentral distance and were recorded by at least five broadband stations. The compiled data set includes 8616 horizontal peak amplitude measurements from 144 broadband stations.

We performed a detailed linear regression analysis to develop the local magnitude formula in accordance with the guidelines of the International Association of Seismology and Physics of the Earth's Interior. As a result, the new local magnitude formula is expressed as: $M_L=\log10(A)+0.9287\log10(R)+0.0012R-1.66$. In addition, we determined the correction factors S for each station.

KEYWORDS: local magnitude; distance correction; attenuation; Mongolia

FUNDING: Not specified.

EDN: RTCLYX

RESEARCH ARTICLE

Correspondence: Baigalimaa Ganbat, baigalaa@iag.ac.mn

Received: September 23, 2025
Revised: November 3, 2025
Accepted: November 14, 2025

FOR CITATION: Ganbat B., Munkhuu U., 2026. Determination of the Local Magnitude Scale (M_L) for Mongolia. Geodynamics & Tectonophysics 17 (1), 0877. doi:10.5800/GT-2026-17-1-0877

ОПРЕДЕЛЕНИЕ ШКАЛЫ ЛОКАЛЬНЫХ МАГНИТУД (M_L) ДЛЯ МОНГОЛИИ

Б. Ганбат, У. Монхоо

Институт астрономии и геофизики МАН, 13343, Улан-Батор, Монголия

АННОТАЦИЯ. Корректировка шкалы локальных магнитуд с учетом региональных тектонических характеристик имеет решающее значение для расширения исследований, направленных на оценку сейсмического риска и измерение сейсмической активности в геодинамических зонах. В данном исследовании разработана шкала локальных магнитуд для территории Монголии. Проанализировано 261 землетрясение с магнитудой >3.5 и эпицентральным расстоянием до 1000 км из монгольского каталога за период с 2012 по 2019 г., зарегистрированное как минимум пятью широкополосными станциями. Собранные данные включают в себя 8616 измерений пиковой амплитуды в горизонтальной плоскости, полученных со 144 широкополосных станций.

Проведен детальный линейный регрессионный анализ для определения формулы локальной магнитуды в соответствии с рекомендациями Международной ассоциации сейсмологии и физики недр Земли. В результате новая формула локальной магнитуды выглядит следующим образом: $M_L=\log10(A)+0.9287\log10(R)+0.0012R-1.66$. Кроме того, были определены поправочные коэффициенты S для каждой станции.

КЛЮЧЕВЫЕ СЛОВА: локальная магнитуда; поправка на расстояние; затухание; Монголия

ФИНАНСИРОВАНИЕ: Не указано.

1. INTRODUCTION

Mongolia is located in East Asia, bordered on the north by the Siberian craton, on the south – by the India-Eurasia collision zone, and on the east – by the Pacific Plate, a remote subduction zone. The collision between the Indian and Eurasian plates and the subduction of the Pacific and Philippine Sea plates have had a profound effect on tectonic deformation in Asia [Wei et al., 2012]. Since 55 million years ago, the Indian Plate has been moving northward, causing the uplift of the Himalayas, the Tibetan Plateau, the Tien Shan, the Altai, and the Sayan Mountains [Molnar, Tapponnier, 1975; Hao et al., 2019]. This movement of the Indian Plate also affects the tectonic evolution of western China and Mongolia. GNSS monitoring of geodynamic activity of Mongolia has revealed the compressional forces exerted by the Indian Plate on the Eurasian Plate, as well as the relative direction and velocity of crustal motion. In western Mongolia, the displacement ranges from 10 mm/year in the southern region to 4 mm/year in the northern region, while the central and eastern regions show an east/southeast displacement at a rate of 4 mm/year [Calais et al., 2003]. As a result, western and central Mongolia are highly seismically active, whereas the eastern and southeastern regions are relatively less active.

The local magnitude (M_L), originally introduced in [Richter, 1935], has become a globally recognized standard and remains one of the most widely used magnitude types in earthquake catalogs. Designed as an empirical method to qualitatively assess earthquake strength, the Richter scale [Richter, 1935] continues to serve as a critical metric in both scientific analyses and real-time public communications. Region-specific calibration of the local magnitude (M_L) scale is critical for improving the reliability of seismic hazard assessments and for enhancing the accuracy of earthquake magnitude estimations in tectonically heterogeneous regions.

In Mongolia, since the installation of seismological stations in 1957, different approaches have been employed to determine the local magnitudes of earthquakes. The energy class K method – an indicator of earthquake strength widely used in the former Soviet Union, Mongolia and Cuba – was applied from 1957 to 2002. Since 2003, local magnitudes have been calculated using the equation developed in [Ulziibat, 2001], which remains in use to the present day. [Ulziibat, 2001] introduced the initial M_L equation, aligning with the Richter scale for Mongolia and stemming from the analysis of earthquake records obtained at short-period stations operated from 1994 to 2000. However, this formula showed a notable dependence on the epicentral distance. A revision in [Mungunsuren, Tatsuhiko, 2013] incorporated data from 143 local and regional earthquakes with magnitudes between 3.5 and 6.7, documented at 23 short-period stations in Mongolia from 2005 to 2012. This update became necessary because of the lack of the data and data quality and due to station instrument response.

Subsequently, the seismic network was modernized, going digital with the inclusion of broadband stations, enhancing the station density in Mongolia, and enabling the use of digital recordings for calculations. These new stations offer increased gain resulting in broader frequency response and dynamic range. Nonetheless, Mongolia still lacks a robust method for developing M_L equation parameters using comprehensive seismic data over an extended duration.

This situation has driven efforts to recalibrate the M_L equation parameters with the utmost accuracy, focusing specifically on Mongolia.

2. DATA AND METHOD

The functioning of the Mongolian seismic network can be categorized into four distinct periods: from the mid-1957s to 1994, characterized by photographic recording; from 1995 to 2005, featuring primary stations with short-period digital instruments alongside photographic recording; from 2005 to 2012, including stations with both short-period and broadband digital instruments; from 2013 onward, marked by the use of short-period, broadband, or accelerometer digital instruments. Since the installation of the first digital seismic station in Mongolia in 1994, there has been a steady increase in the number of digital short-period stations.

To increase seismic activity monitoring and expand seismological studies in Mongolia, numerous short-period seismometers were upgraded to high-sensitivity broadband seismometers between 2013 and 2015. The number of seismic stations in Mongolia has increased annually, with the current infrastructure comprising 35 permanent broadband stations (depicted as yellow triangles in Fig. 1), along with numerous mini-arrays and five regional digital three-component short-period seismometers. In the Ulaanbaatar area, sixteen of these broadband stations are equipped with CMG-3ESPC (60 and 120 s) broadband seismometers by Güralp Inc., featuring a sensitivity of 2000 V/m/s. A CMG-DM24S3EAM data logger (Güralp Inc.) is linked to each sensor. All stations consistently capture seismic data at a sampling rate of 50 Hz. The Mongolian seismic network consists of stations distributed throughout the country, transmitting real-time data to the Mongolian National Data Center at the Institute of Astronomy and Geophysics in Ulaanbaatar, Mongolia. Additionally, as part of the Central Mongolian Seismic Experiments [Meltzer et al., 2019], temporary broadband seismic arrays utilizing IRIS-PASSCAL instruments were set up in western Mongolia, such as the Govi-Altay region (14 stations) and the Khovsgol region (26 stations) between August 2014 and March 2016, and in the Hangay Dome area (72 stations) from June 2012 to July 2014 (depicted as blue triangles in Fig. 2). These temporary broadband seismic stations used the STS-2 seismometers and Quanterra Q330 digitizers with a sampling frequency of 100 Hz. By incorporating local data from both temporary and permanent broadband seismic stations, totaling 144 stations, installed and operated throughout Mongolia, we have developed a local magnitude formula.

2.1. Data selection

We analyzed around 20000 amplitude data from the Mongolia seismic catalog for the period 2012–2019, using recordings from 144 broadband stations. The selection

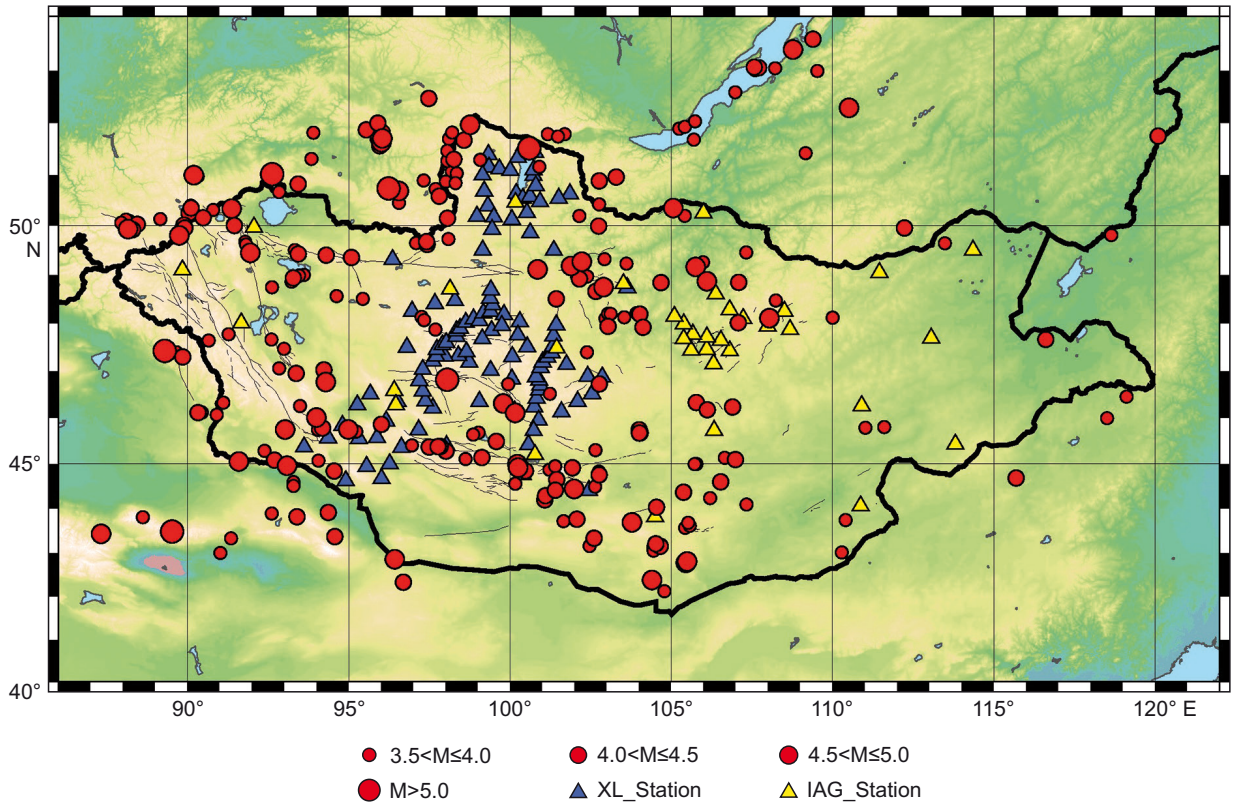

Fig. 1. The stations and earthquakes used in this study.
Yellow triangles indicate permanent seismic stations, blue triangles indicate temporary seismic stations, and red circles represent the earthquakes used in this study.

Рис. 1. Станции и землетрясения, использованные в данном исследовании.
Желтые треугольники – постоянные сейсмические станции, синие треугольники – временные сейсмические станции, красные кружочки – землетрясения, использованные в данном исследовании.

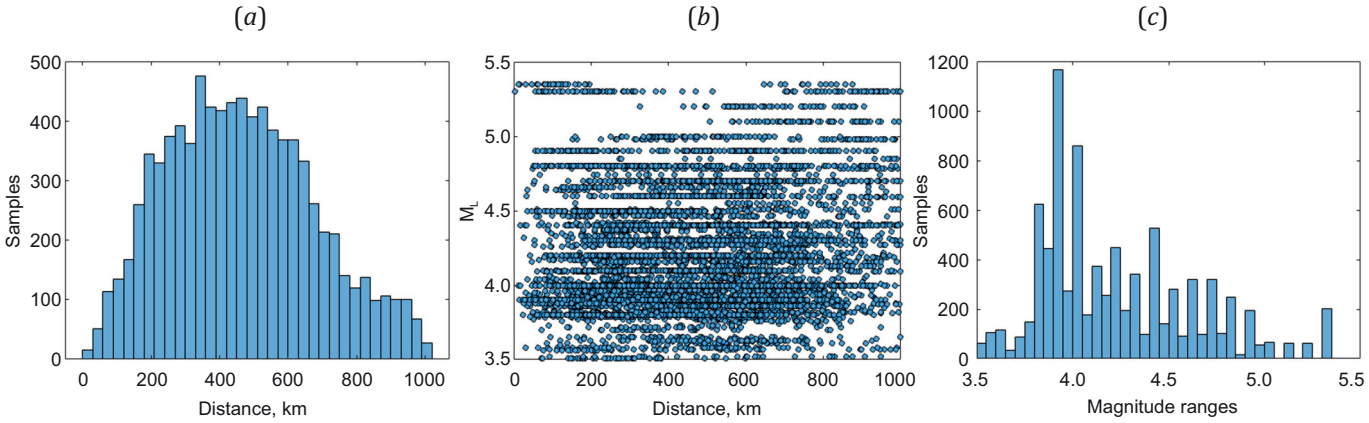

Fig. 2. Earthquake dataset used in this study.
(*a*) – distribution of samples (horizontal waveform amplitudes) with respect to hypocentral distance; (*b*) – magnitude distribution as a function of distance; (*c*) – sample distribution across different magnitude ranges.

Рис. 2. Данные о землетрясениях, использованные в настоящем исследовании.
(*a*) – распределение выборок (амплитуд горизонтальных волн) относительно гипоцентрального расстояния; (*b*) – распределение магнитуды как функции расстояния; (*c*) – распределение выборок по различным диапазонам магнитуд.

criteria included local magnitudes (M_L) between 3.5 and 5.6, a signal-to-noise ratio greater than 1.5, epicentral distances less than 1,000 km, and recordings from at least five stations per event. Based on these criteria, 261 seismic events were selected, resulting in a final dataset comprising 8616 amplitude records. Fig. 2, a illustrates the sample distribution relative to epicentral distance, Fig. 2, b illustrates the magnitude (M_L) relative to epicentral distance, and Fig. 2, c presents the distribution of the event samples as a function of M_L.

Initially, all original waveforms were deconvolved with their respective instrument responses. Subsequently, the frequency response of the Wood – Anderson torsion seismograph for displacement was convolved, following the procedure described in [Uhrhammer, Collins, 1990], as this response has been adopted in the IASPEI standard procedures [IASPEI, 2005, 2013].

2.2. Method

The M_L scale, tailored for southern California's shallow quakes, incorporated an epicentral distance correction as outlined in [Richter, 1935] and revised in [Richter, 1958]. [Richter, 1935] introduced a local magnitude calculated using the logarithm (log$A$) of the maximum trace amplitude (A) in millimeters. This measurement was taken using the horizontal components of a standard Wood – Anderson seismometer with specified parameters: a free period T=0.8 s, magnification 2800, and a damping factor 0.8 [Anderson, Wood, 1925]. According to [Richter, 1935] scale, an event with M_L=0 at 100 km epicentral distance produces a peak amplitude of 0.001 mm on a standard Wood – Anderson seismograph when S=0 and, similarly, an M_L=3 event yields a peak amplitude of 1 mm at 100 km. Using the original Richter relation (Equation 1) as a foundation, we employed the method introduced in [Hutton, Boore, 1987] to define the empirical distance correction function for calculating M_L,

$$M_L=\log10A(R)-\log10A_0(R)+S, \quad (1)$$

$$-\log10A_0=a\log10A(R/100)-b(R-100)+3 \quad (2)$$

where $\log10A(R)$ represents the observed zero-to-peak amplitude in millimeters in a WA seismogram, $-\log A_0$ is the empirical distance correction, S is the empirically derived station correction, R is the epicentral distance in kilometers, and a and b are the respective empirical coefficients for geometric spreading and anelastic attenuation specific to the region. A constant 3 is added to adhere to the initial Richter M_L definition. To develop the new magnitude scale, we blend equations (1) and (2) to yield a precise distance-correction function as

$$M_{Li}-S_j-a\cdot\log10(R_{ij}/100)-b(R_{ij}-100)=\log10A_{ij}+3;$$
$$i=1,2,...m;\ j=1,2,...n \quad (3)$$

where A_{ij} is the maximum horizontal zero-to-peak amplitude of the i th event at the j th station, M_{Li} is the magnitude of the ith event, S_j is the station correction of the j th station, R_{ij} is the hypocentral distance from the ith event to the jth station, m is number of events, and n is number of stations. Equation (3) can be written in a standard matrix form as $Gm=d$, which represents a typical linear inversion prolem in geophysics that can be soved using the least squares method from [Alsaker et al., 1991; Miao, Langston, 2007; Nguyen et al., 2011].

The G-matrix, which consists of real values and is non-singular, has dimensions $(m\times n+1)\times(m+n+2)$, where $m\times n$ corresponds to the total number of amplitude measurements in the dataset. The linear system can be solved using the inverse of G. To ensure solution uniqueness, we apply a constraint that the sum of station corrections for a given event must be zero $\left(\sum_{j=1}^{n} S_j = 0\right)$, as these corrections are only defined relative to each other [Menke, 2018].

The inverse matrix is computed using singular value decomposition [Press et al., 2007; Menke, 2018].

3. RESULTS AND DISCUSSION

For a total of 8616 amplitude data, converted to Wood – Anderson seismograms, 144 stations throughout Mongolia recorded 261 earthquakes with magnitudes greater than M_L 3.5 and epicentral distances ranging from 3 to 1000 km. To reduce the influence of outlying measurements defined by large residuals relative to the initial distance corrections derived from preliminary linear inversions, we applied an iterative outlier rejection procedure. Specifically, measurements with absolute residuals greater than 0.6 were considered outliers, corresponding to approximately two standard deviations (2σ) from the mean residual. Equation (2) was then solved repeatedly, starting with the full dataset of 8,616 measurements. After three iterations, a total of 170 measurements were identified as outliers and excluded from the final solution. Fig. 3, a presents the values of as a function of distance following the initial outlier removal step. Data points that fall outside of the specified bounds are marked with a blue line. Fig. 3, b shows the corresponding residual distribution at this stage. Fig. 3, c, d display the same types of plots: residuals versus distance and residual distribution, respectively, but for the final iteration, after all outliers had been identified and removed. The final distance correction functions were calculated in Equation (4) using these data and the methodology provided:

$$\log10(A_0)=0.9287\log10(R/100)+0.0012(R-100)+3. \quad (4)$$

Based on defined distance correction functions, the magnitude formulas were converted to use amplitude measurements in nanometers and are expressed by Equation (5) as follows:

$$M_L=\log10(A)+0.9287\log10(R)+0.0012R-1.66 \quad (5)$$

where A is the peak amplitude in nanometers as per a Wood – Anderson sensor simulation, and R is the hypocentral distance in kilometers.

Additionally, the regression analysis identified the station corrections, which are shown in App. 1, Table 1.1. Station correction factors were calculated to account for

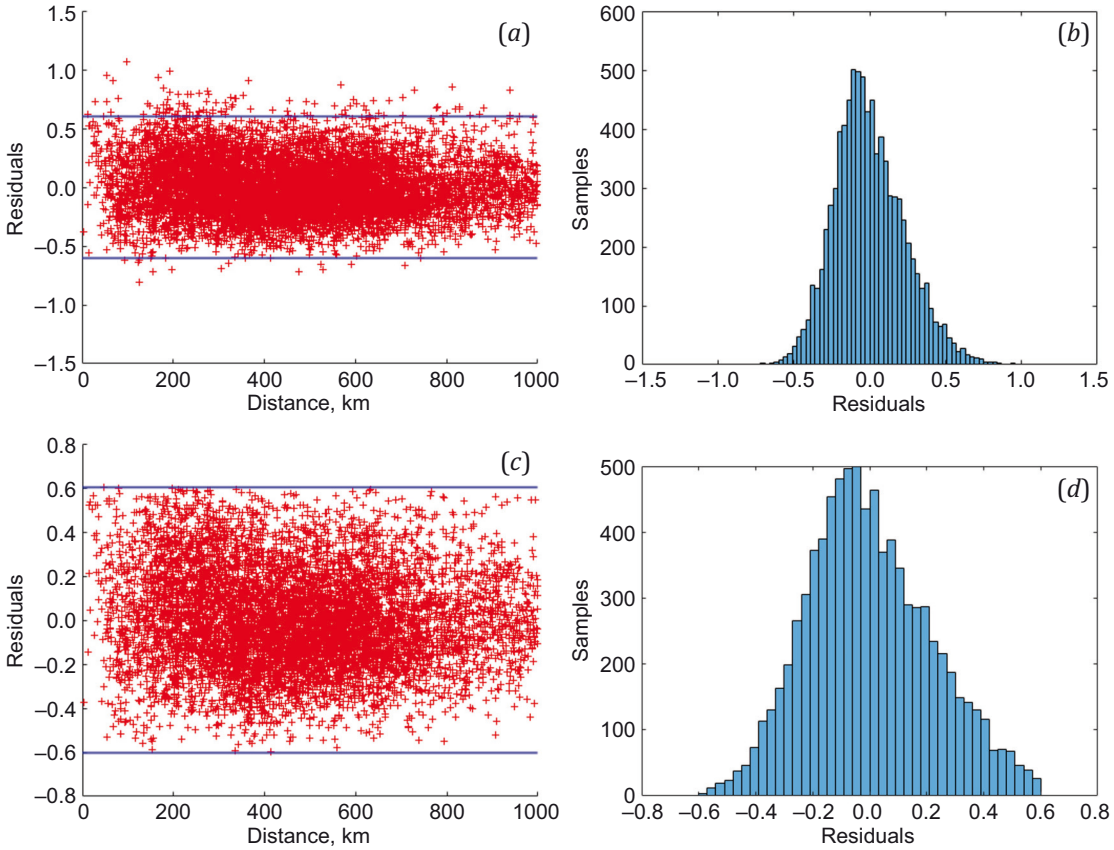

Fig. 3. Residuals distribution.
(*a*) – results from the first iteration of the outlier removal procedure using the initial dataset, where red plus symbols outside the blue lines indicate residuals identified as outliers, and the blue lines represent the thresholds for defining outliers; (*b*) – residual distribution after the first step; (*c*) – results from the final iteration after outlier removal; (*d*) – residual distribution at the final step.

Рис. 3. Распределение остатков.
(*a*) – результаты первой итерации метода удаления выбросов с использованием исходного набора данных, где красные знаки «плюс» за пределами синих линий обозначают остатки, идентифицированные в качестве выбросов, а синие линии представляют пороговые значения для определения выбросов; (*b*) – распределение остатков после первого шага; (*c*) – результаты последней итерации после удаления выбросов; (*d*) – распределение остатков на последнем шаге.

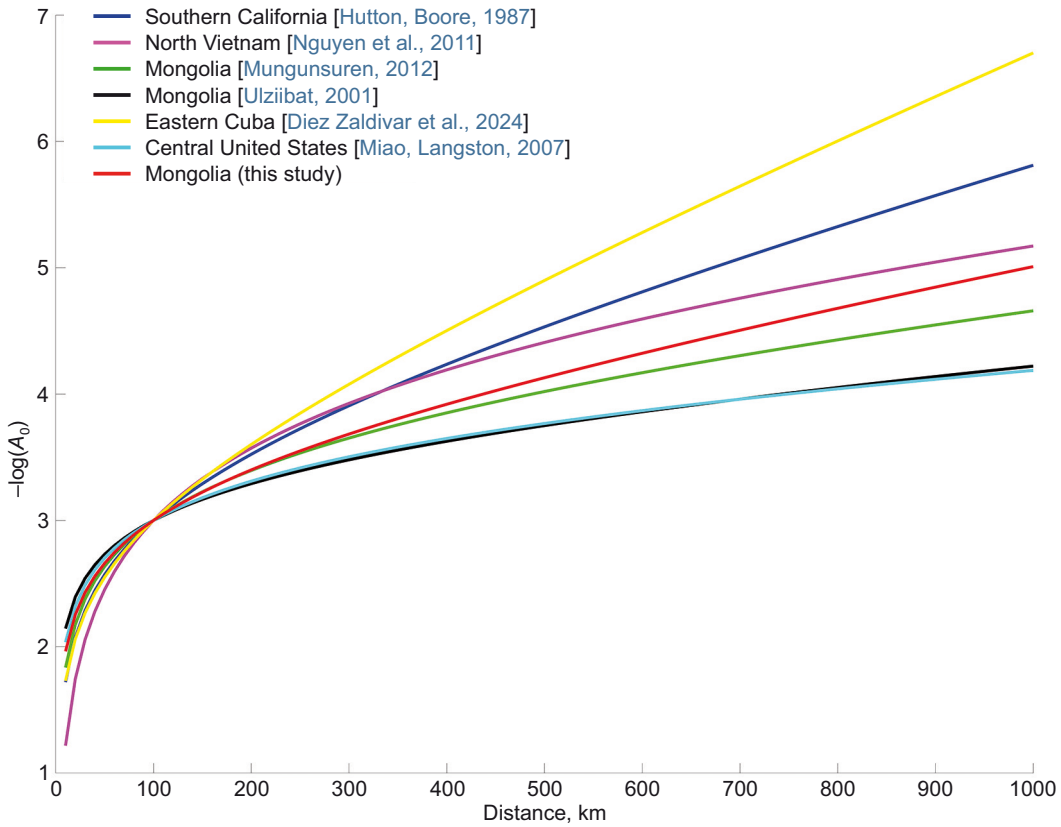

Fig. 4. Calibration functions for M_L determination in Mongolia and other regions.

Рис. 4. Калибровочные функции для определения M_L в Монголии и других регионах.

the local geological conditions at each station, with values ranging from –0.68 to +0.28. Fig. 4 illustrates distance correction functions derived from several regions: Southern California [Hutton, Boore, 1987], Northern Vietnam [Nguyen et al., 2011], Mongolia [Ulziibat, 2001; Mungunsuren, Tatsuhiko, 2013], Eastern Cuba [Diez Zaldivar et al., 2024], the central United States [Miao, Langston, 2007], and Mongolia (this study). Comparison of these functions indicates that the attenuation parameter *b* obtained in this study is higher than that reported for the central United States and the two previous magnitude scales for Mongolia. This increased value likely reflects greater seismic wave energy dissipation in the study area. Besides, as shown in Fig. 4, the distance correction curve derived in this study falls within two curves proposed for Northern Vietnam and Mongolia in [Mungunsuren, Tatsuhiko, 2013].

4. CONCLUSIONS

In this research, we derived new M_L scales for the horizontal component, using a dataset of 8446 amplitude readings from 261 earthquakes recorded between 2012 and 2019 at 144 broadband stations. These data enabled us to derive empirical coefficients for geometrical spreading and anelastic attenuation, which are essential for correcting the amplitude as a function of distance.

Station correction factors were also determined, reflecting local geological conditions beneath each station. The station corrections ranged from –0.68 to +0.28.

The new M_L scales offer more consistent magnitude estimations than the scale currently used in IAG's routine seismic analysis. Based on these improvements, we recommend adopting the proposed M_L scales to replace the existing local magnitude scale used by the IAG.

5. ACKNOWLEDGEMENTS

The authors are grateful to everyone involved in the collection of seismic data for this research. We also thank the Institute of Astronomy and Geophysics of the Mongolian Academy of Sciences and the IRIS Data Management Center for their provision of seismic waveform data.

6. CONTRIBUTION OF THE AUTHORS

Baigalimaa Ganbat plays a key role in data curation, formal analysis, inquiry, software use, scripting, visualization, and primary paper drafting. The data resource was revised and edited by Ulziibat Munkhuu.

7. DISCLOSURE

The authors declare that they have no conflicts of interest relevant to this manuscript.

8. REFERENCES

Alsaker A., Kvamme L.B., Hansen R.A., Dahle A., Bungum H., 1991. The ML Scale in Norway. Bulletin of the Seismological Society of America 81 (2), 379–398. https://doi.org/10.1785/BSSA0810020379.

Anderson J.A., Wood H.O., 1925. Description and Theory of the Torsion Seismometer. Bulletin of the Seismological Society of America 15 (1), 1–72. https://doi.org/10.1785/BSSA0150010001.

Calais E., Vergnolle M., Sankov V., Lukhnev A., Miroshnichenko A., Amarjargal S., Déverchère J., 2003. GPS Measurements of Crustal Deformation in the Baikal-Mongolia Area (1994–2002): Implications on Current Kinematics of Asia. Journal of Geophysical Research: Solid Earth 108 (B10), 2501. https://doi.org/10.1029/2002JB002373.

Diez Zaldivar E.R., Sandron D., Cutie Mustelier M., 2024. Calibration of the Local Magnitude Scale (ML) for Eastern Cuba. Seismological Research Letters 95 (2A), 791–803. https://doi.org/10.1785/0220230286.

Hao M., Li Y., Zhuang W., 2019. Crustal Movement and Strain Distribution in East Asia Revealed by GPS Observations. Scientific Reports 9, 16797. https://doi.org/10.1038/s41598-019-53306-y.

Hutton L.K., Boore D.M., 1987. The M_L Scale in Southern California. Bulletin of the Seismological Society of America 77 (6), 2074–2094. https://doi.org/10.1785/BSSA0770062074.

IASPEI, 2005. Summary of Magnitude Working Group Recommendations on Standard Procedures for Determining Earthquake Magnitudes from Digital Data. Available from: http://download.iaspei.org/commissions/CSOI/summary_of_WG_recommendations_2005.pdf (Last Accessed September 10, 2025).

IASPEI, 2013. Summary of Magnitude Working Group Recommendations on Standard Procedures for Determining Earthquake Magnitudes from Digital Data. Available from: http://download.iaspei.org/commissions/CSOI/Summary_WG_recommendations_20130327.pdf (Last Accessed September 10, 2025).

Meltzer A., Stachnik J.C., Sodnomsambuu D., Munkhuu U., Tsagaan B., Dashdondog M., Russo R., 2019. The Central Mongolia Seismic Experiment: Multiple Applications of Temporary Broadband Seismic Arrays. Seismological Research Letters 90 (3), 1364–1376. https://doi.org/10.1785/0220180360.

Menke W., 2018. Geophysical Data Analysis: Discrete Inverse Theory. 4th Ed. Academic Press, London, 322 p. https://doi.org/10.1016/C2016-0-05203-8.

Miao Q., Langston C.A., 2007. Empirical Distance Attenuation and the Local-Magnitude Scale for the Central United States. Bulletin of the Seismological Society of America 97 (6), 2137–2151. https://doi.org/10.1785/0120060188.

Molnar P., Tapponnier P., 1975. Cenozoic Tectonics of Asia: Effects of a Continental Collision. Science 189 (4201), 419–426. https://doi.org/10.1126/science.189.4201.419.

Mungunsuren D., Tatsuhiko H., 2013. Local Magnitude Scale for Mongolia and Determination of Mwp and Ms (BB). Bulletin of the International Institute of Seismology and Earthquake Engineering 47, 31–36.

Nguyen L.M., Lin T.-L., Wu Y.-M., Huang B.-S., Chang C.-H., Huang W.-G., Le T.S., Dinh V.T., 2011. The First M_L Scale for North of Vietnam. Journal of Asian Earth Sciences 40 (1), 279–286. https://doi.org/10.1016/j.jseaes.2010.07.005.

Press W.H., Teukolsky S.A., Vetterling W.T., Flannery B.P., 2007. Numerical Recipes: The Art of Scientific Computing. 3rd Ed. Cambridge University Press, New York, 1256 p. https://doi.org/10.1142/S0218196799000199.

Richter C.F., 1935. An Instrumental Earthquake Magnitude Scale. Bulletin of the Seismological Society of America 25, 1–32.

Richter C.F., 1958. Elementary Seismology. W.H. Freeman, San Francisco, 578 p.

Uhrhammer R.A., Collins E.R., 1990. Synthesis of Wood-Anderson Seismograms from Broadband Digital Records. Bulletin of the Seismological Society of America 80 (3), 702–716. https://doi.org/10.1785/BSSA0800030702.

Ulziibat M., 2001. Local Magnitude Scale for Mongolia. Annual Report of 2001. Department of Seismology, IAG, MAS, 6 p.

Wei W., Xu J., Zhao D., Shi Y., 2012. East Asia Mantle Tomography: New Insight Into Plate Subduction and Intraplate Volcanism. Journal of Asian Earth Sciences 60, 88–103. https://doi.org/10.1016/j.jseaes.2012.08.001.

APPENDIX 1

Table 1.1. Stations corrections
Таблица 1.1. Станционные поправки

Station	Latitude	Longitude	Elevation	Station correction	Station	Latitude	Longitude	Elevation	Station correction
ALM	46.58	96.408	999	0.138	HD46	46.83	100.06	2068	–0.097
ALTM	46.28	96.463	2374	–0.106	HD48	46.21	97.608	1803	0.178
AT01	45.36	93.616	1561	0.267	HD49	46.35	97.373	1793	–0.367
AT02	45.56	94.362	2113	–0.439	HD50	46.57	97.295	1838	–0.142
AT03	45.83	94.806	1671	–0.187	HD51	46.80	97.188	2174	–0.009
AT04	46.27	95.267	1020	–0.243	HD52	47.03	97.294	2650	0.115
AT05	46.51	95.669	1705	0.255	HD54	47.50	96.803	1846	0.155
AT06	46.35	96.511	2047	–0.260	HD56	47.40	98.651	2567	0.248
AT07	45.93	96.159	1424	–0.215	HD59	48.25	96.964	2251	0.278
AT08	45.56	95.876	2056	0.129	HD60	48.41	97.673	1946	0.138
AT09	44.93	95.557	1861	0.209	HD61	48.47	98.295	1846	–0.217
AT10	44.62	94.907	1390	–0.028	HD62	48.18	99.813	2077	0.207
AT12	44.66	96.014	1596	0.187	HD63	47.96	99.744	2169	0.106
AT13	44.99	96.270	1091	–0.471	HD64	48.03	100.30	1960	0.064
AT14	45.36	96.636	2289	0.257	HD65	47.75	100.24	2058	0.047
AT15	45.74	97.167	1279	–0.444	HD66	46.81	98.087	2256	–0.179
BANB	49.10	89.843	2188	–0.013	HD67	46.35	99.051	2192	0.111
BGDM	45.20	100.77	2188	0.187	HD68	44.40	102.44	1707	–0.253
BULM	48.82	103.52	999	–0.005	HD69	44.75	100.40	1609	–0.446
CCBM	47.48	101.45	1737	–0.105	HD70	45.39	98.029	2352	–0.059
DABM	49.50	114.36	821	–0.037	HD71	45.55	95.317	1915	0.146
DADM	49.05	111.45	1022	0.000	HD72	48.74	103.64	1190	–0.060
DARM	45.42	113.81	1249	–0.678	HD73	49.50	101.36	1168	–0.336
DOM	47.69	113.06	999	0.016	HD74	49.50	99.152	1495	–0.320
DZBM	43.81	104.50	1557	–0.125	HD75	49.31	96.357	1896	0.137
ERM	44.06	110.87	1202	0.125	HTGM	50.46	100.17	1662	–0.031
GALM	46.26	110.90	1261	0.111	HV01	51.39	99.332	1539	–0.135
HBD	48.01	91.669	144	0.172	HV02	51.15	99.35	1546	–0.067
HD01	46.87	102.86	1714	–0.060	HV03	50.99	99.15	1639	–0.134
HD02	46.89	102.41	1633	–0.302	HV04	50.68	99.197	1699	0.153
HD03	46.52	102.55	1878	0.072	HV05	50.38	99.313	1828	0.107
HD04	46.35	102.09	2210	–0.197	HV06	50.18	98.976	1617	0.193
HD05	46.12	101.59	2010	0.029	HV07	51.11	99.668	1568	0.025
HD06	46.23	100.75	1895	–0.233	HV08	51.08	100.01	1751	–0.256
HD07	45.94	100.89	1700	0.121	HV09	50.16	99.502	1980	0.241
HD08	45.72	100.73	1576	–0.187	HV10	51.57	100.45	1685	–0.113
HD09	45.41	100.57	1401	–0.138	HV13	50.63	100.19	1678	0.187
HD10	46.42	100.83	2084	–0.200	HV14	50.46	100.17	1663	0.066
HD11	46.59	100.91	2233	0.034	HV15	50.11	100.06	1569	0.082
HD12	46.69	100.94	2360	–0.076	HV17	50.54	100.40	1692	0.149
HD13	46.80	100.90	2534	–0.250	HV18	50.57	100.62	1696	0.163
HD14	46.88	100.81	2516	0.074	HV19	50.98	100.73	1683	0.069
HD15	47.07	100.95	2186	–0.004	HV20	51.10	100.73	1703	0.014
HD16	47.19	101.01	2018	–0.124	HV21	51.43	100.78	1677	0.247

Table 1.1 (continued)
Таблица 1.1 (продолжение)

Station	Latitude	Longitude	Elevation	Station correction	Station	Latitude	Longitude	Elevation	Station correction
HD17	47.28	101.16	1908	0.026	HV22	50.25	100.52	1663	0.199
HD18	47.38	101.29	1807	–0.432	HV23	49.92	99.447	1889	0.250
HD19	47.51	101.32	1788	–0.013	HV24	49.85	100.63	1566	0.232
HD21	47.97	101.43	1776	0.029	HV25	50.47	100.93	1305	–0.033
HD22	47.13	101.75	1839	0.004	HV26	50.62	101.86	1158	–0.317
HD23	47.51	100.53	2033	–0.169	HV27	50.54	101.51	1140	–0.225
HD24	47.31	100.07	2255	0.092	HV31	51.34	100.24	1693	–0.350
HD25	47.01	99.399	2058	0.201	HV32	50.79	100.80	1723	0.233
HD26	47.18	98.736	2557	0.268	MDGM	45.72	106.33	1414	0.013
HD27	47.32	98.401	2547	0.175	SHBM	50.24	106.00	99	0.098
HD28	47.31	97.976	2525	0.232	TSCM	48.71	98.14	1839	0.005
HD29	47.21	97.604	2157	–0.066	U01M	48.10	107.23	1854	–0.109
HD30	47.31	97.712	2279	0.111	U02M	48.25	108.51	1526	–0.035
HD31	47.45	97.732	2300	0.194	U03M	47.94	107.99	1858	–0.008
HD32	47.55	97.903	2365	0.205	U04M	47.87	108.68	155	–0.021
HD33	47.59	98.022	2601	0.224	U05M	47.42	106.82	1768	0.022
HD34	47.73	98.336	2568	0.103	U06M	47.64	106.54	1475	0.069
HD35	47.84	98.340	2452	0.085	U07M	47.15	106.31	1545	0.066
HD36	47.89	98.448	2313	0.215	U08M	47.46	106.10	1444	0.028
HD37	48.02	98.627	2329	0.110	U09M	47.71	106.10	1444	0.035
HD38	48.09	98.868	2253	0.215	U10M	47.43	105.62	134	0.085
HD39	48.05	99.052	2262	0.231	U11M	47.78	105.67	1383	0.107
HD40	48.21	99.175	2185	0.094	U12M	47.68	105.38	134	0.112
HD41	48.24	99.400	2183	–0.092	U13M	47.99	105.39	1324	0.004
HD42	48.38	99.461	1857	–0.039	U14M	48.14	105.10	1421	–0.085
HD43	48.52	99.382	1701	0.143	U15M	48.61	106.38	1072	0.093
HD44	47.85	99.428	2138	0.071	U16M	48.28	106.81	1269	–0.138
HD45	47.68	99.140	2292	–0.226	ULBM	49.96	92.062	955	0.011